

Mechanistic Analysis of Circuit Preservation in Federated Learning

Muhammad Haseeb¹ Salaar Masood¹ Muhammad Abdullah Sohail¹

GitHub Repository:

<https://github.com/ha405/FedMI>

Abstract

Federated Learning (FL) enables collaborative training of models on decentralized data, but its performance degrades significantly under Non-IID (non-independent and identically distributed) data conditions. While this accuracy loss is well-documented, the internal mechanistic causes remain a black box. This paper investigates the canonical FedAvg algorithm through the lens of Mechanistic Interpretability (MI) to diagnose this failure mode. We hypothesize that the aggregation of conflicting client updates leads to **circuit collapse**, the destructive interference of functional, sparse sub-networks responsible for specific class predictions. By training inherently interpretable, weight-sparse neural networks within an FL framework, we identify and track these circuits across clients and communication rounds. Using Intersection-over-Union (IoU) to quantify circuit preservation, we provide the first mechanistic evidence that Non-IID data distributions cause structurally distinct local circuits to diverge, leading to their degradation in the global model. Our findings reframe the problem of statistical drift in FL as a concrete, observable failure of mechanistic preservation, paving the way for more targeted solutions.

1. Introduction

Federated Learning (FL) allows for training machine learning models on decentralized data, which addresses privacy and communication concerns by keeping raw data on local devices (McMahan et al., 2017). The standard algorithm,

¹Department of Computer Science, Lahore University of Management Sciences. Correspondence to: Muhammad Abdullah Sohail <26100142@lums.edu.pk>, Muhammad Haseeb <26100253@lums.edu.pk>, Salaar Masood <26100149@lums.edu.pk>.

Proceedings of the 42nd International Conference on Machine Learning, Vancouver, Canada. PMLR 267, 2025. Copyright 2025 by the author(s).

Federated Averaging (FedAvg), builds a global model by averaging the weights of models trained locally. While FedAvg works well on independently and identically distributed (IID) data, its performance drops significantly when client data is Non-IID (Zhao et al., 2018). Most existing research analyzes this failure from a statistical perspective, often referring to "weight divergence." However, the internal structural changes that cause the global model to fail remain unclear.

We analyze the model's internal structure using Mechanistic Interpretability (MI). We focus specifically on identifying circuits, defined as the minimal set of parameters and distinct computational steps required to perform a specific task. In standard dense models, these circuits are difficult to isolate because of superposition (Elhage et al., 2022). Because the network compresses many features into few dimensions, individual neurons become polysemantic, participating in multiple unrelated circuits simultaneously and obscuring the model's underlying logic

Recent work shows that enforcing weight sparsity during training can solve this problem. While the Lottery Ticket Hypothesis showed that sparse sub-networks exist within dense models (Frankle & Carbin, 2019), newer methods train models to be sparse from the start. This sparsity acts as a constraint that forces the model to learn distinct, disentangled circuits that are easier to identify (Gao et al., 2025). Unlike pruning used for compression (Han et al., 2015), we use sparsity here as a tool to analyze the model's structure.

In this paper, we apply these circuit-level analysis techniques to the internal dynamics of FedAvg for the first time. We hypothesize that the performance drop on Non-IID data is caused by **circuit collapse**, the degradation of structural integrity in functional sub-networks due to the averaging of conflicting client updates. Our work shows this phenomenon manifests in two distinct failure modes: **structural drift**, where a circuit's function is preserved but its topology is altered, and **destructive interference**, where competing circuits overwrite each other, leading to functional collapse. This hypothesis provides a structural explanation for the statistical problem of weight divergence (Zhao et al., 2018).

We focus on two primary research questions:

- **RQ1 (Inter-Client Consistency):** Do distinct clients

independently learn the same circuits for the same class, and how does this change under FedAvg?

- **RQ2 (Intra-Client Stability):** How do a specific client’s circuits change over time as global updates are integrated?

By answering these questions for both IID and Non-IID settings, we aim to show that circuit collapse is a primary cause of failure in federated learning.

The rest of the paper is organized as follows. Section 2 outlines our FL framework, sparse training method, and circuit discovery process. Section 3 presents our findings using Intersection-over-Union (IoU) metrics to measure circuit consistency. Section 4 analyzes the implications of these results, and Section 5 concludes the paper.

2. Methodology

Our empirical study is designed to mechanistically analyze the effects of federated averaging on neural circuits. We establish a baseline under IID data conditions before extending our analysis to more complex Non-IID scenarios. All experiments are conducted in a PyTorch based simulated Federated environment on RTX 4090.

2.1. Experimental Setup

Architecture and Dataset. We use a simple 3-layer Convolutional Neural Network (CNN), optimized for tractability and mechanistic analysis. The model consists of three convolutional layers (32, 64, and 128 channels respectively), each followed by ReLU activation and Max-Pooling, and a fully-connected layer for classification. All experiments are performed on the MNIST dataset.

Federated Learning Configuration. For our IID baseline, we simulate a federated network of $K = 5$ clients over $T = 10$ communication rounds. The MNIST training dataset is shuffled and partitioned evenly among the clients, ensuring each client’s local data distribution is representative of the global IID distribution. In each round, all clients participate in training, performing $E = 5$ local epochs with a batch size of $B = 256$ before their model updates are aggregated by the central server using FedAvg (McMahan et al., 2017).

2.2. Sparse Training and Circuit Discovery

To achieve interpretability, we use weight sparsity to expose the model’s inner workings as sparsity forces the model to learn compact, isolated circuits. (Gao et al., 2025) The process within each client’s local training phase involves two sequential stages: sparse network training and circuit discovery.

Phase A: Sparse Training. We first train the CNN with a structural sparsity constraint. Formally, we seek to minimize the pretraining loss \mathcal{L}_{pre} subject to a global constraint on the number of non-zero parameters k :

$$\min_{\theta} \mathcal{L}_{\text{pre}}(\theta) \quad \text{s.t.} \quad \|\theta\|_0 \leq k \quad (1)$$

Following each gradient update, we apply iterative magnitude pruning to enforce this target weight sparsity (e.g., 99% for the IID case) (Han et al., 2015). This step is not for model compression, but rather to act as a strong regularizer that removes redundant pathways and forces the network to converge on efficient, stable sub-networks. This aligns with the finding that sparsity acts as an interpretable inductive bias (Gao et al., 2025), which limits the solution space and discourages superposition, compelling the model to implement behaviors through distinct, disentangled circuits. To avoid dead neurons, we enforce a minimum of $j = 4$ nonzero weights per neuron vector \mathbf{w}_n :

$$\|\mathbf{w}_n\|_0 \geq 4 \quad \forall n \in \text{neurons} \quad (2)$$

This constraint, consistent with the sparse training methods referenced (Gao et al., 2025), maintains sufficient connectivity to support signal flow during the circuit discovery phase.

Phase B: Circuit Discovery. After local sparse training, we identify the functional circuits for specific classes. With the network weights θ frozen, we learn a set of binary masks \mathbf{m} for the convolutional layer channels. We parameterize these masks via learnable scores τ , where $\mathbf{m} = H(\tau)$ is the Heaviside step function. We optimize τ using a Straight-Through Estimator (STE) to approximate the gradient through the discrete step. This process minimizes a joint objective composed of the task-specific cross-entropy loss and an L_0 regularization term penalized by a coefficient λ :

$$\min_{\tau} (\mathcal{L}_{\text{task}}(x, y; \theta \odot H(\tau)) + \lambda \|H(\tau)\|_0) \quad (3)$$

This objective identifies the minimal sub-network of neurons sufficient for classifying a target class. During this discovery phase, pruned neurons are subject to zero-ablation (where $m_i = 0$). The resulting set of active neurons and their connecting weights constitute the discovered “circuit” for a given class

2.3. Circuit Analysis and Metrics

To answer our research questions, we quantify the structural similarity between discovered circuits using the Intersection-over-Union (IoU) metric. For any two circuits, defined by their sets of active neurons (C_1, C_2) in a given layer, the IoU is computed as:

$$\text{IoU}(C_1, C_2) = \frac{|C_1 \cap C_2|}{|C_1 \cup C_2|}$$

An IoU of 1.0 indicates perfect structural identity, while an IoU of 0 indicates complete disjointness. We apply this metric to assess two key properties:

Inter-Client Consistency: To measure how circuits for the same class differ across clients, we compute the average pairwise IoU between the circuits discovered by all clients within the same communication round.

Intra-Client Stability: To track how circuits evolve for a single client, we compute the IoU between a client’s circuit in round t and its circuit in round $t + 1$.

2.4. Non-IID Experimental Design

To investigate the impact of statistical heterogeneity, we design several Non-IID data distributions. These include pathological “extreme skew” scenarios where each client’s dataset is restricted to samples from only one, two, or three classes. We also conduct ablation studies across different levels of weight sparsity to analyze its influence on circuit preservation. The specific configurations for each Non-IID experiment are detailed in their respective results sections.

3. Results

Our mechanistic study proceeds in two phases. First, we establish a baseline for circuit behavior under ideal IID data conditions. Second, we introduce Non-IID data distributions to test our central hypothesis of circuit collapse.

3.1. Circuit Preservation in the IID Setting

In the IID setting, where all clients learn from statistically similar data, our results confirm that FedAvg successfully preserves and reinforces a single, canonical circuit for each class.

Inter-Client Consistency. We first examine whether different clients independently discover similar circuits. Figure 1 shows the average pairwise IoU for circuits across all 5 clients. The results demonstrate high consistency: for all classes and all layers, the average IoU remains near 1.0 throughout the training process. This implies that despite training on distinct data shards, all clients converge on structurally identical circuits. We attribute this to the extreme 99% weight sparsity, which acts as a powerful regularizer to significantly restrict the solution space. When combined with a shared initialization and identical data distributions, this constraint effectively compels the optimization trajectories of all clients to converge on the same unique and efficient sub-network for the task. This quantitative result is qualitatively confirmed by a visual overlay of the final circuits from two clients, which shows near-total overlap (see Appendix, Figure 11).

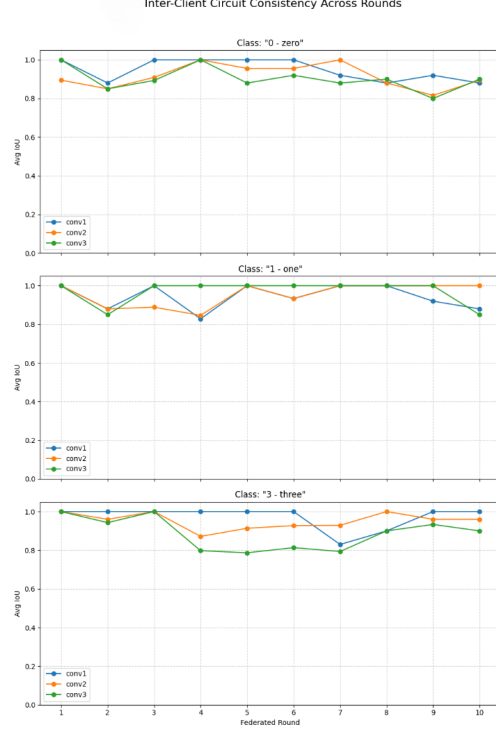


Figure 1. Inter-Client Circuit Consistency (IID). The average pairwise IoU between circuits for the same class across all 5 clients remains near 1.0, indicating convergence to a single, canonical circuit structure.

Intra-Client Stability. We also observe high stability within individual clients across rounds. As shown in the Appendix (Figure 10), circuit stability quickly converges to 1.0 after the initial aggregation rounds. This persistence is visually corroborated by comparing the topology of a client’s circuit between late training rounds (see Appendix, Figure 12), where the structure remains virtually identical with only minor edge refinements (e.g., the pruning of 3 connections between Round 9 and 10), reinforcing that learned mechanisms are stable over time.

Local-to-Global Circuit Preservation. A crucial test of FedAvg is whether the circuits discovered locally are preserved in the final aggregated global model. Figure 2 plots the IoU between a client’s local circuit and the corresponding circuit discovered in the global model. The similarity rapidly converges to an IoU near 1.0. This finding is significant: it shows that the FedAvg process does not introduce structural drift in the IID setting. The features learned by the local model are not just functionally preserved but are also maintained at the same structural locations in the global model. This structural fidelity is visually apparent in the overlay of a client’s local circuit against the global model’s circuit (see Appendix, Figure 13), where shared connections dominate the topology.

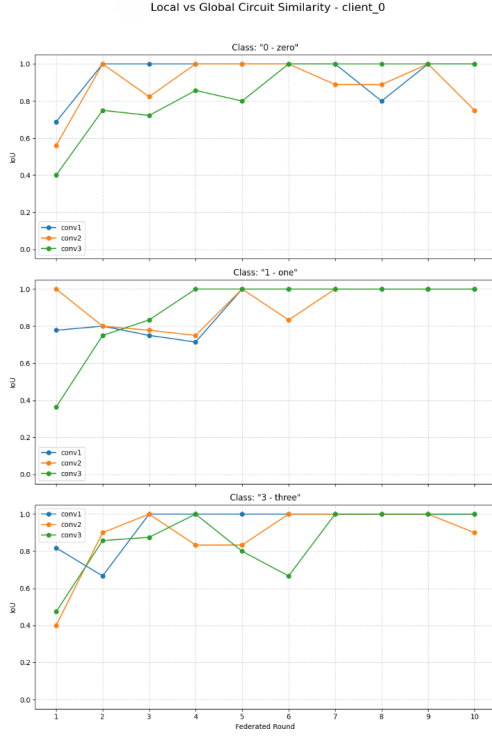


Figure 2. Local vs. Global Circuit Similarity (IID, Client 0). The IoU between Client 0’s local circuit and the corresponding global circuit rapidly approaches 1.0, demonstrating that FedAvg preserves circuit structure without introducing drift.

3.2. Circuit Divergence and Collapse under Non-IID Conditions

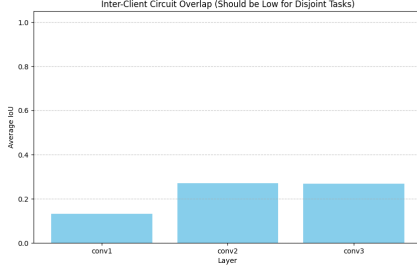


Figure 3. Inter-Client Circuit Overlap (Non-IID, 1-Class per Client). The average IoU between circuits from specialist clients is low, indicating they learn structurally disjoint sub-networks.

Having established the IID baseline, we now introduce statistical heterogeneity. We analyze three extreme label skew scenarios: a 1-class-per-client, a 2-class-per-client, and a 3-class-per-client distribution. We also study an intermediate case where clients share one common class and have two distinct classes, to examine how a shared label affects circuit formation. Since the local task complexity is reduced when

clients observe fewer labels, we enforce a stricter sparsity constraint of 99.5%. In this setting, each client acts as a “specialist” on a disjoint set of classes.

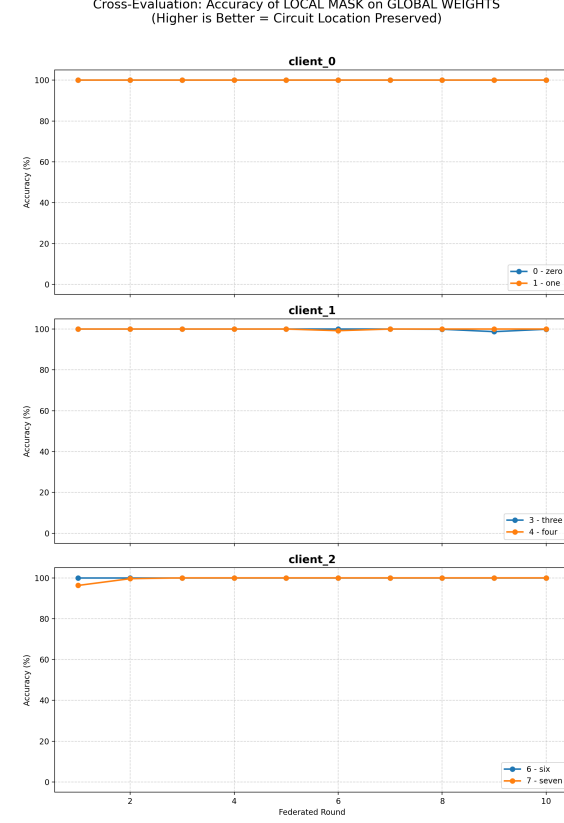


Figure 4. Cross-Evaluation Accuracy (Non-IID, 2-Class per Client). Applying a client’s local circuit mask to the global model yields near-perfect accuracy on its specialized classes, indicating functional preservation.

Structural Divergence. The immediate consequence of this partitioning is profound structural divergence. Figure 3 shows the average inter-client circuit overlap for the 1-class experiment. In stark contrast to the IID case, the IoU between specialist clients is extremely low (below 0.3 for all layers). This quantitatively confirms that clients learning different tasks discover entirely different, non-overlapping sub-networks. This finding holds for the 2-class experiment as well (see Appendix, Figure 14).

Functional Preservation without Structural Identity. A surprising result emerges when we test the functional validity of these divergent circuits. We perform a cross-evaluation by applying a client’s final local circuit mask onto the final global model’s weights. Figure 4 shows that for both specialist experiments, the local mask achieves nearly 100% accuracy on its corresponding target class. This indicates that while the global model’s overall performance is poor, the specialized knowledge from each client is not

entirely destroyed. The global model successfully integrates the disjoint circuits in a way that preserves their *functional* capability. In this uniform skew setting, FedAvg appears to perform a form of modular knowledge composition rather than complete destructive interference.

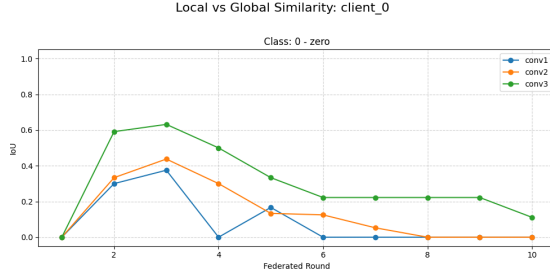


Figure 5. Local vs. Global Circuit Similarity (Non-IID, 1-Class, Client 0). The structural IoU between the local and global circuit for class “0” peaks early and then decays, demonstrating that the client’s original circuit structure is not preserved.

Evidence of Structural Collapse. While the function of a local circuit remains viable, its original structure is not maintained in the global model. Figure 5 plots the structural similarity (IoU) between a client’s local circuit and the corresponding circuit in the global model. A consistent pattern of collapse is observed: the IoU peaks in an early round before steadily declining as conflicting updates from other specialist clients are averaged in. This demonstrates that the global model resolves the conflicting updates by moving the computation to a different sub-network, confirming that the original local circuit structure is overwritten and “collapses.” This structural drift is the mechanistic underpinning of the weight divergence identified in prior work (Zhao et al., 2018). This trend is consistent across all clients and experiments (see Appendix, Figures 15 and 16).

3.2.1. DESTRUCTIVE INTERFERENCE IN OVERLAPPING NON-IID DISTRIBUTIONS

We next analyze a more complex Non-IID scenario with 3 disjoint classes per client, extending the experiment to 50 rounds to observe long-term dynamics. In this setup (e.g., Client 0 sees classes {0,1,2}, Client 1 sees {3,4,5}), the task distributions are still disjoint, but the increased complexity per client forces the learning of more diverse features.

Increased Structural Overlap and Competition. Unlike the highly specialized 1-class and 2-class experiments, this setup induces a significantly higher degree of structural overlap between the circuits learned by different clients. Figure 6 shows that the average inter-client IoU is now much higher, ranging from 0.6 to nearly 0.9. This suggests that as clients learn more complex, multi-class distributions, they begin to converge on shared low-level feature detectors, leading their circuits to compete for the same neural substrate.

Functional Instability and Circuit Dominance. This increased competition leads to functional instability, a key departure from the simpler Non-IID cases. Figure 7 plots the cross-evaluation accuracy over 50 rounds. Instead of maintaining a stable 100% accuracy, the performance of local masks on the global model becomes highly volatile. For any given client, the accuracy frequently plummets to 0% for several rounds before recovering.

This provides direct evidence of **destructive interference**. The training logs confirm this phenomenon: in many rounds, the “Local Mask on Global Weights Acc” is 0.00% for a majority of classes, while one or two circuits remain functional. This suggests a “winner-take-all” dynamic where the FedAvg update in a given round aligns the global model with the circuit of one dominant client, temporarily rendering the circuits from other clients non-functional. This constant overwriting prevents the global model from achieving a stable, multi-specialist state and is a core mechanism behind its poor overall performance.

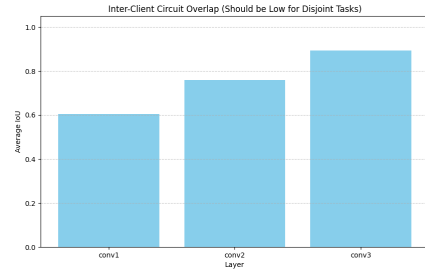


Figure 6. Inter-Client Circuit Overlap (Non-IID, 3-Class per Client). The higher IoU compared to simpler disjoint settings indicates that clients are attempting to use the same neurons, creating a potential for conflict during aggregation.

Persistent Structural Flux. The functional instability is mirrored by a persistent lack of structural convergence. Figure 8 shows that the IoU between local and global circuits remains low and noisy throughout all 50 rounds, never achieving the stability seen in the IID case. This confirms that the global model is in a constant state of flux, with each round’s aggregation partially overwriting the structural features established by the previous one. This sustained structural collapse prevents the emergence of a coherent, universal set of circuits. The same noisy, low-IoU pattern is observed for all clients in this experiment (see Appendix, Figure 17).

3.2.2. THE STABILIZING EFFECT OF A SHARED CLASS

Finally, we investigate a hybrid scenario to bridge our findings from the IID and disjoint Non-IID experiments. In this setup, all clients are trained on a single *shared class* (“0”) while also being specialists on two *distinct classes* (e.g., Client 0 sees {0, 1, 2}, Client 1 sees {0, 3, 4}, etc.). This

experiment directly tests whether the presence of a common learning objective can mitigate the destructive interference observed previously.

The results, shown in Figure 9, reveal a clear dichotomy in circuit behavior.

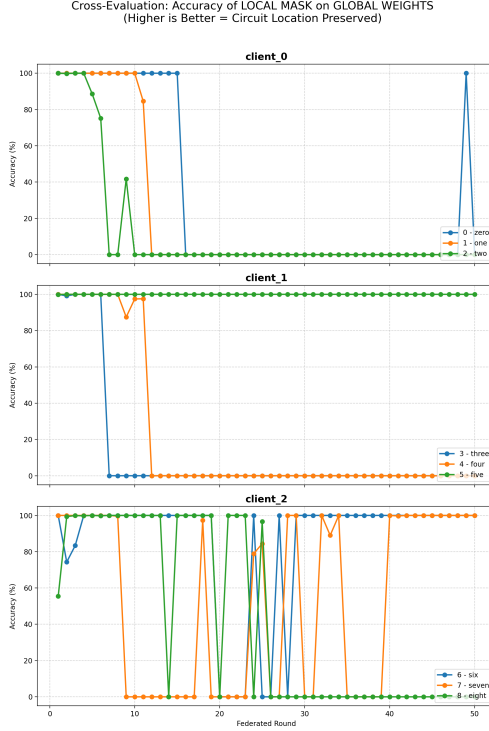


Figure 7. Cross-Evaluation Accuracy (Non-IID, 3-Class per Client, 50 Rounds). The accuracy of local masks on the global model is highly volatile, frequently dropping to 0%, which indicates destructive interference between competing client circuits during aggregation.

Preservation of the Shared Circuit. For the shared class ("0"), the cross-evaluation accuracy of the local mask on the global model remains consistently at or near 100% across all clients and all rounds. This demonstrates that when all clients train on the same task, their circuit updates are harmonious. FedAvg successfully aggregates these updates, leading to a stable, canonical circuit for the shared class that is functionally valid for all clients, mirroring the behavior observed in the fully IID setting.

Continued Interference for Distinct Circuits. In stark contrast, the circuits for the distinct, specialist classes (e.g., "1" and "2" for Client 0) exhibit the same functional volatility seen in the purely disjoint experiments. Their cross-evaluation accuracy frequently collapses to 0%, recovering only when the stochasticity of the aggregation process happens to favor their structure.

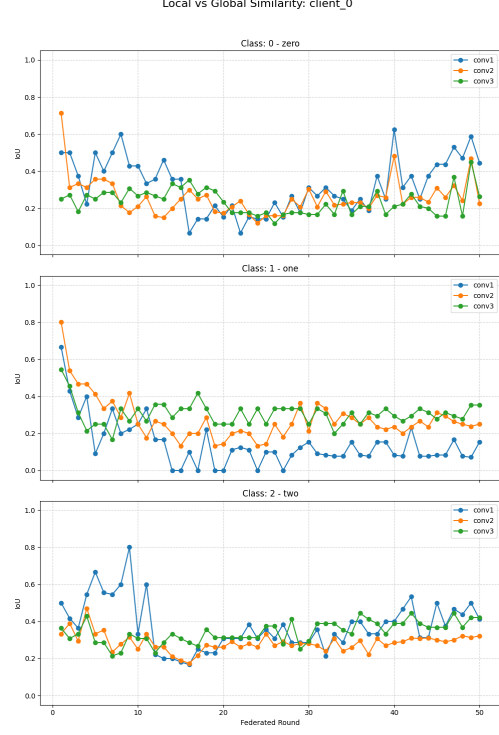


Figure 8. Local vs. Global Circuit Similarity (Non-IID, 3-Class, Client 0). The IoU remains low and erratic for 50 rounds, showing no convergence and confirming a state of persistent structural collapse.

This experiment provides the most compelling evidence for our hypothesis: **circuit collapse is a direct consequence of conflicting updates**. When updates align (for the shared class), circuits are preserved. When they conflict (for the distinct classes), they interfere destructively. This confirms that the statistical properties of the data distribution at the client level have a direct and predictable mechanistic impact on the structural integrity of the resulting global model. The structural dynamics for all classes are detailed in the Appendix (Figure 18).

3.3. Sparsity as a Mitigator of Destructive Interference

To directly test the **Constraint Hypothesis** in the Non-IID setting, we conduct an ablation study on the 2-class-per-client experiment across four levels of target weight sparsity: 95%, 97%, 99%, and 99.5%. We hypothesize that higher sparsity, by reducing the available parameters, will force clients to converge on more compact and structurally consistent circuits, thereby mitigating the destructive interference observed during aggregation.

Our findings, presented in Figure 19 in the Appendix, reveal a clear, monotonic relationship between the degree of sparsity and the functional stability of the global model.

At the lowest sparsity level (95%), the system exhibits chaotic interference. The cross-evaluation accuracy is highly volatile, with frequent, unpredictable collapses across multiple clients and classes. By the final round, half of the specialist circuits (3 out of 6) have failed entirely, demonstrating that the less constrained models learn large, overlapping circuits that conflict severely during aggregation.

As we increase the sparsity constraint to 97% and 99%, a significant improvement in stability is observed. The chaotic flickering is replaced by more controlled dynamics. While circuit failures still occur, they are less frequent, and the surviving circuits stabilize much more quickly. For instance, at 99% sparsity, most functional circuits are stable by round 5, a marked improvement over the chaotic behavior at 95%.

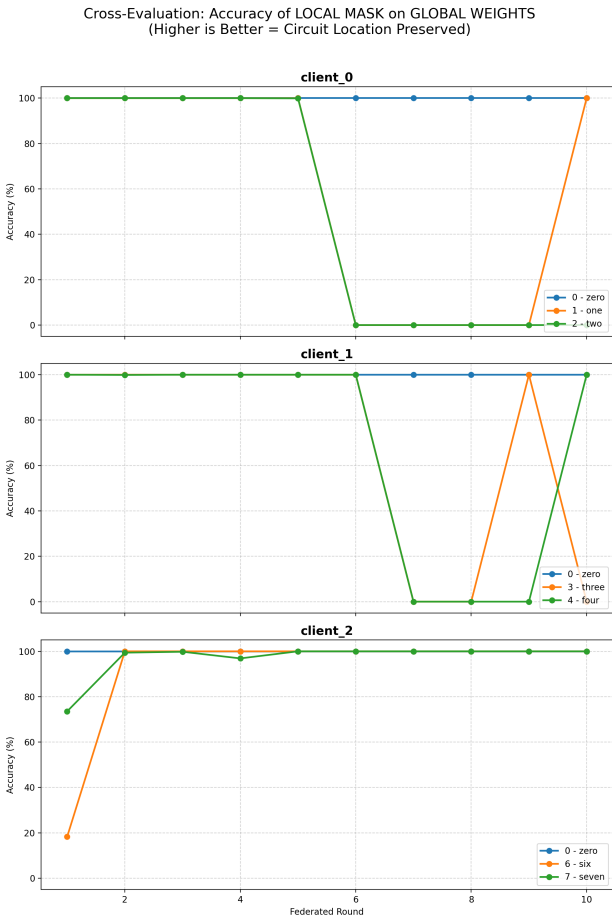


Figure 9. Cross-Evaluation Accuracy with a Shared Class. For the shared class ("0", blue line), accuracy is stable at 100% across all clients. For the distinct classes (e.g., "1" and "2", orange and green lines), accuracy is volatile and frequently collapses, demonstrating destructive interference.

Finally, at the highest sparsity level of 99.5%, the system

approaches a state of stable preservation. Destructive interference is minimal, with only one circuit failing permanently while the others remain almost perfectly functional throughout the training process.

This progression provides strong evidence that weight sparsity acts as a powerful regularizer against divergent updates in Non-IID federated learning. By severely constraining the solution space, higher sparsity forces clients to discover more canonical and compact circuits. This increased structural agreement reduces the magnitude of destructive interference during averaging, leading to a more functionally coherent global model.

4. Discussion

Our results provide a mechanistic characterization of the failure modes of Federated Averaging under Non-IID conditions. By leveraging weight sparsity as an analytical tool, we move beyond statistical metrics of weight divergence to observe the structural degradation of functional sub-networks. Our findings yield critical insights into the internal dynamics of decentralized learning and suggest new directions for designing more robust aggregation algorithms.

From Weight Divergence to Circuit Collapse. A primary contribution of our work is the mechanistic re-framing of "weight divergence" as **circuit collapse**. Prior work identifies this phenomenon as a statistical drift of parameter vectors (Zhao et al., 2018). Our findings reveal this drift is not an amorphous shift but a concrete structural event. Under IID conditions, the inductive bias of sparsity guides all clients to a single, canonical circuit, which FedAvg reinforces. Under Non-IID conditions, however, clients learn disjoint circuits, leading to two distinct failure modes during aggregation: (1) **Modular Addition with Structural Drift**, where specialist functions are preserved but relocated to different neurons in the global model, and (2) **Destructive Interference**, where competing circuits overwrite each other, causing functional volatility and collapse.

Sparsity as a Regularizer Against Interference. Our ablation study demonstrates that weight sparsity is more than an interpretability tool; it is a powerful regularizer against interference. We observed a clear monotonic relationship: as sparsity increases, functional stability improves. Less constrained models (e.g., 95% sparsity) learn larger, overlapping circuits that conflict severely. By enforcing extreme sparsity (e.g., 99.5%), we compel clients to find more minimal and orthogonal sub-networks. This reduces the surface area for destructive interference, suggesting that future FL algorithms could benefit from explicit sparsity constraints to improve robustness.

Implications for Aggregation Strategies. The persistence of circuit collapse implies that naive coordinate-wise averag-

ing (as performed in FedAvg) is fundamentally ill-suited for Non-IID regimes where topological alignment is not guaranteed. Our results suggest two distinct algorithmic pathways for improvement. First, post-hoc alignment strategies, such as neuron permutation or matching, may be required to align functional circuits before averaging. Second, and perhaps more fundamentally, our findings advocate for preventing circuit collision by design. Future algorithms could enforce orthogonality constraints during local training, explicitly forcing clients to encode unique features into disjoint sub-networks. By ensuring that clients utilize non-overlapping sets of neurons for conflicting tasks, destructive interference could be mechanically eliminated during the global aggregation phase. Additionally, the "Shared Class" experiment demonstrates that partial data overlap stabilizes specific sub-circuits; this supports the case for Modular Federated Learning, where shared knowledge is aggregated while task-specific circuits remain local.

Implications for Polysemanticity in Federated Learning. Our findings suggest that FedAvg can be a source of **induced polysemanticity**. In a single model, polysemanticity arises when many concepts are compressed into few neurons. In FedAvg, a similar process occurs at the network level: when the global model averages a "cat" circuit from Client A and a "dog" circuit from Client B that use the same neurons, the resulting global neurons become polysemantic, tasked with representing conflicting features. The functional volatility we observe is a direct symptom of this, as the global model struggles to disentangle these merged concepts.

Limitations and Future Work. Our analysis was conducted on a tractable CNN architecture and the MNIST dataset. Validating these findings on more complex models and datasets is a critical next step. Future work could also develop a formal quantitative relationship between statistical data skew (e.g., EMD) and the rate of IoU degradation. Finally, our results motivate the exploration of circuit-aware aggregation algorithms that move beyond naive averaging to explicitly align or preserve functional sub-networks.

5. Conclusion

In this paper, we conducted a mechanistic analysis of Federated Averaging, providing the first direct, structural evidence for its performance degradation on Non-IID data. By training interpretable sparse models, we demonstrated that the statistical problem of weight divergence manifests as a physical phenomenon of **circuit collapse**. Our key findings are threefold: (1) Under IID conditions, FedAvg successfully preserves a single, canonical circuit across all clients. (2) Under Non-IID conditions, clients learn disjoint circuits that suffer from either structural drift or destructive interference during aggregation. (3) Increasing model sparsity

acts as a potent regularizer, mitigating this interference and improving the functional stability of the global model. Our work reframes the challenge of Non-IID learning in FL as a problem of mechanism preservation and opens the door to developing new, circuit-aware aggregation strategies that are robust by design.

References

Elhage, N., Hume, T., Olsson, C., Schiefer, N., Henighan, T., Kravec, S., Hatfield-Dodds, Z., Lasenby, R., Drain, D., Chen, C., et al. Toy models of superposition. *arXiv preprint arXiv:2209.10652*, 2022.

Frankle, J. and Carbin, M. The lottery ticket hypothesis: Finding sparse, trainable neural networks. In *International Conference on Learning Representations (ICLR)*, 2019.

Gao, L., Rajaram, A., Coxon, J., Govande, S. V., Baker, B., and Mossing, D. Weight-sparse transformers have interpretable circuits. *arXiv preprint arXiv:2511.13653*, 2025.

Han, S., Pool, J., Tran, J., and Dally, W. J. Learning both weights and connections for efficient neural networks. In *Advances in Neural Information Processing Systems 28 (NIPS 2015)*, 2015.

McMahan, H. B., Moore, E., Ramage, D., Hampson, S., and Arcas, B. A. y. Communication-efficient learning of deep networks from decentralized data. In *Proceedings of the 20th International Conference on Artificial Intelligence and Statistics (AISTATS)*, volume 54 of *Proceedings of Machine Learning Research*, 2017.

Zhao, Y., Li, M., Lai, L., Suda, N., Civin, D., and Chandra, V. Federated learning with non-iid data. *arXiv preprint arXiv:1806.00582*, 2018.

A. Supplementary Figures

This appendix provides supplementary figures that support the findings presented in the main text.

A.1. Supplementary Figures for IID Experiments

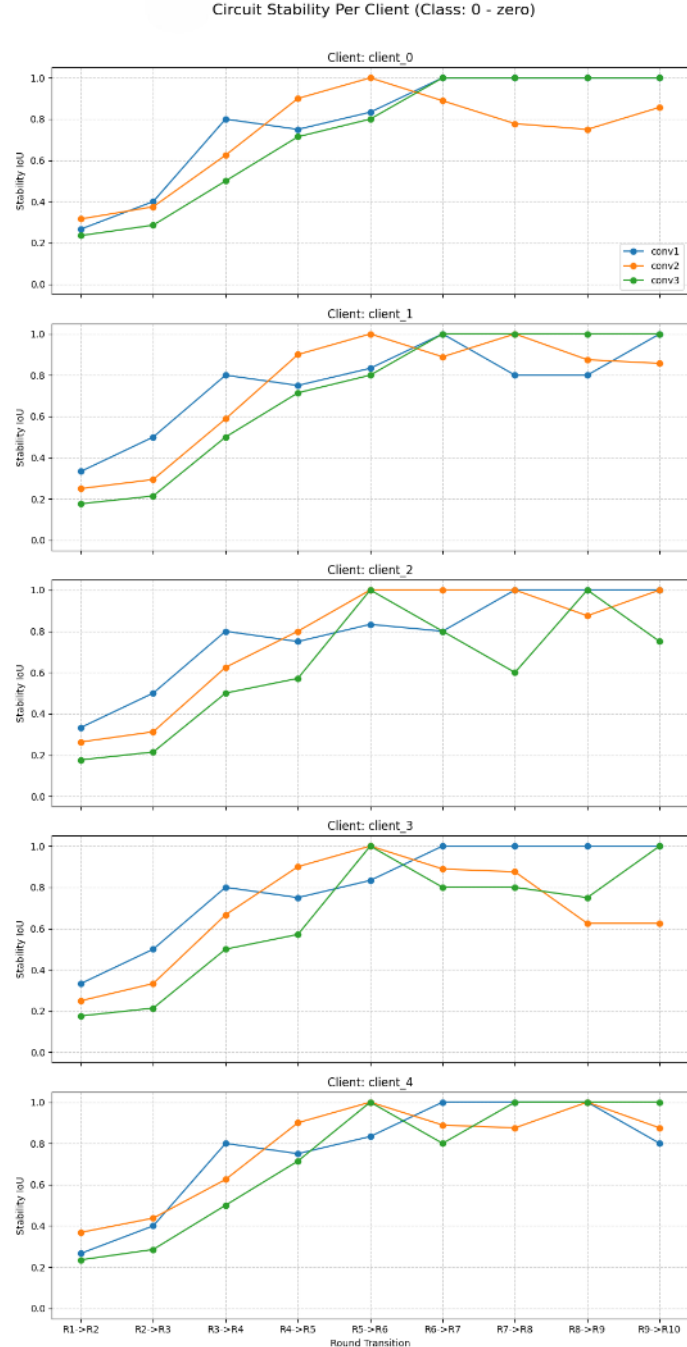


Figure 10. Supplementary Figure: Intra-Client Stability (IID). Intra-client stability quickly reaches an IoU of 1.0, demonstrating that circuits do not change significantly after the initial communication rounds.

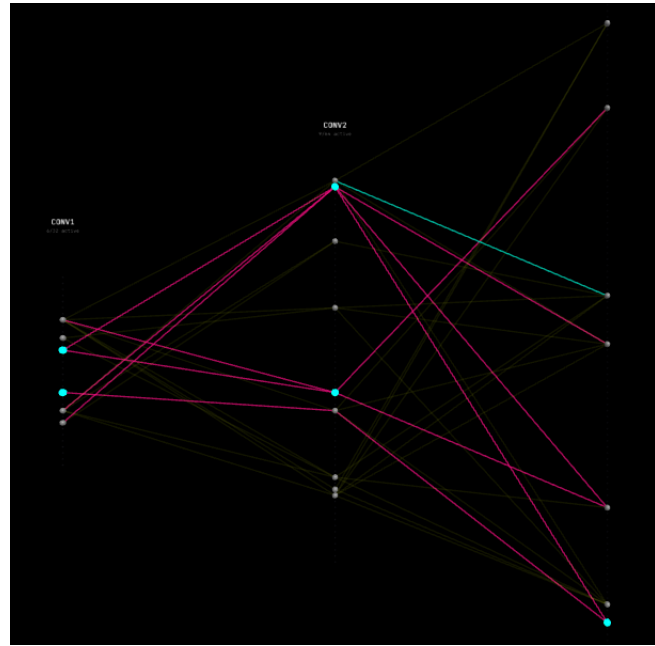


Figure 11. Supplementary Figure: Qualitative Circuit Overlay (IID). A visual overlay of the final circuits for Class "0" from Client 0 and Client 4 shows near-perfect structural alignment, with the vast majority of components being shared (grey).

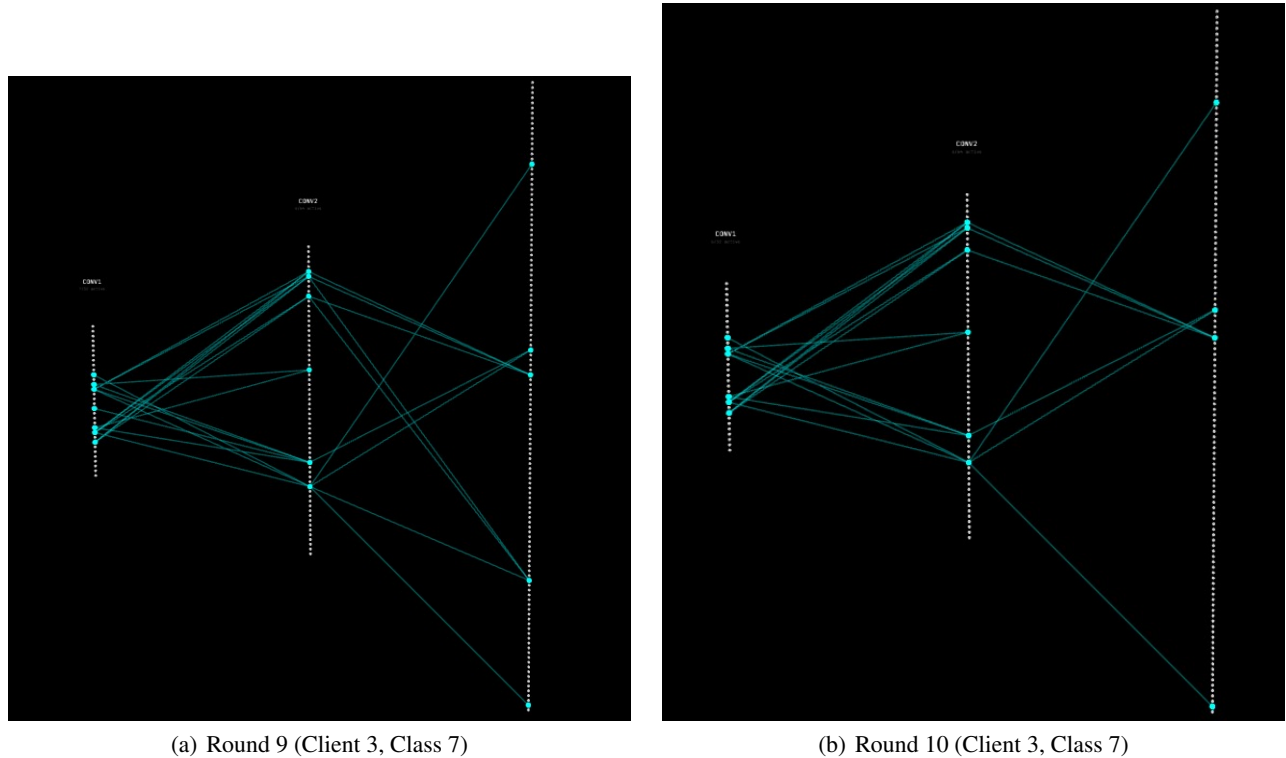


Figure 12. Supplementary Figure: Visualizing Intra-Client Stability (IID). A direct comparison of the circuit for Client 3 (Class 7) between Round 9 and Round 10. The topology remains visually identical with only a minor refinement (the removal of 3 connections in Round 10), reinforcing the quantitative finding that circuits stabilize and persist within clients.

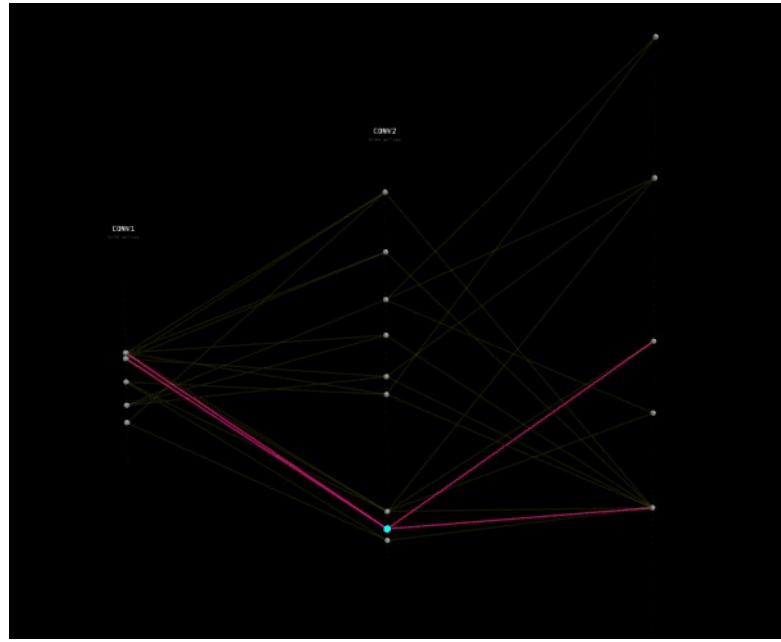


Figure 13. Supplementary Figure: Visualizing Local-to-Global Preservation (IID). An overlay of Client 1's local circuit vs. the Global model's circuit for Class "0". The dominance of shared edges (grey) indicates that the aggregated global model has successfully preserved the exact structure learned locally by the client, without introducing drift.

A.2. Supplementary Figures for Non-IID Experiments

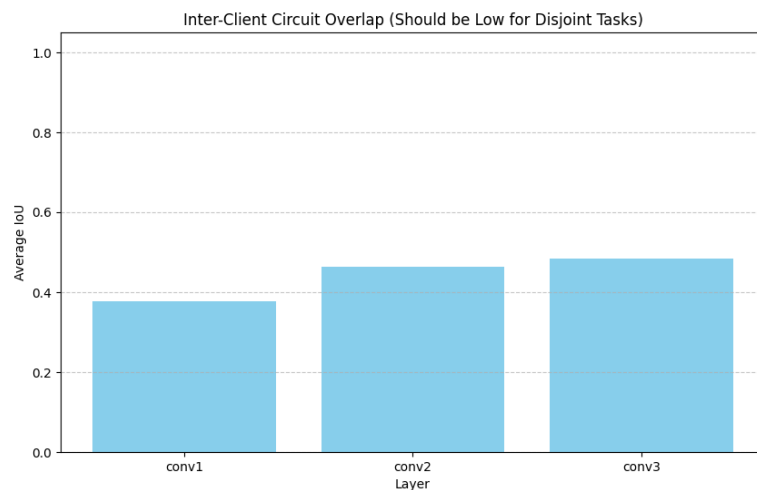


Figure 14. Supplementary Figure: Inter-Client Circuit Overlap (Non-IID, 2-Class per Client). Consistent with the 1-class experiment, the average IoU between circuits from specialist clients remains low, confirming structural divergence.

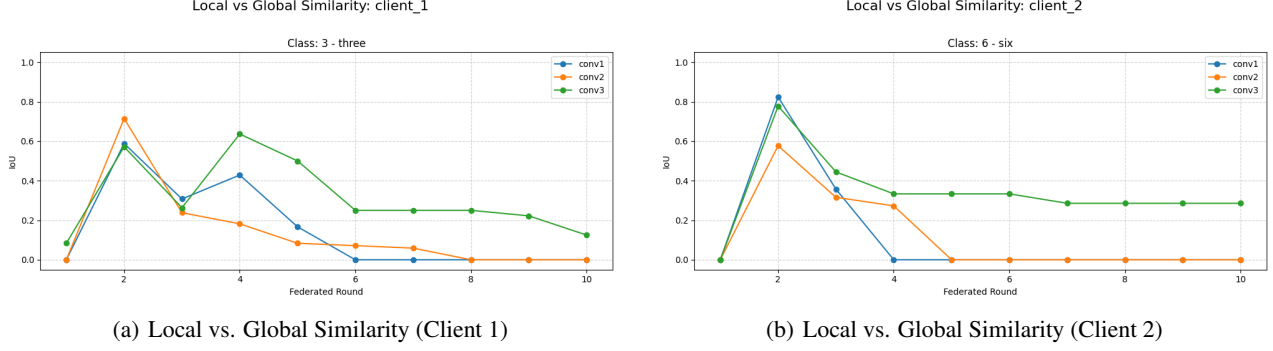


Figure 15. Supplementary Figure: Local vs. Global Circuit Similarity for Clients 1 and 2 (Non-IID, 1-Class per Client). The pattern of structural collapse, where IoU peaks early and then decays, is consistent across all specialist clients.

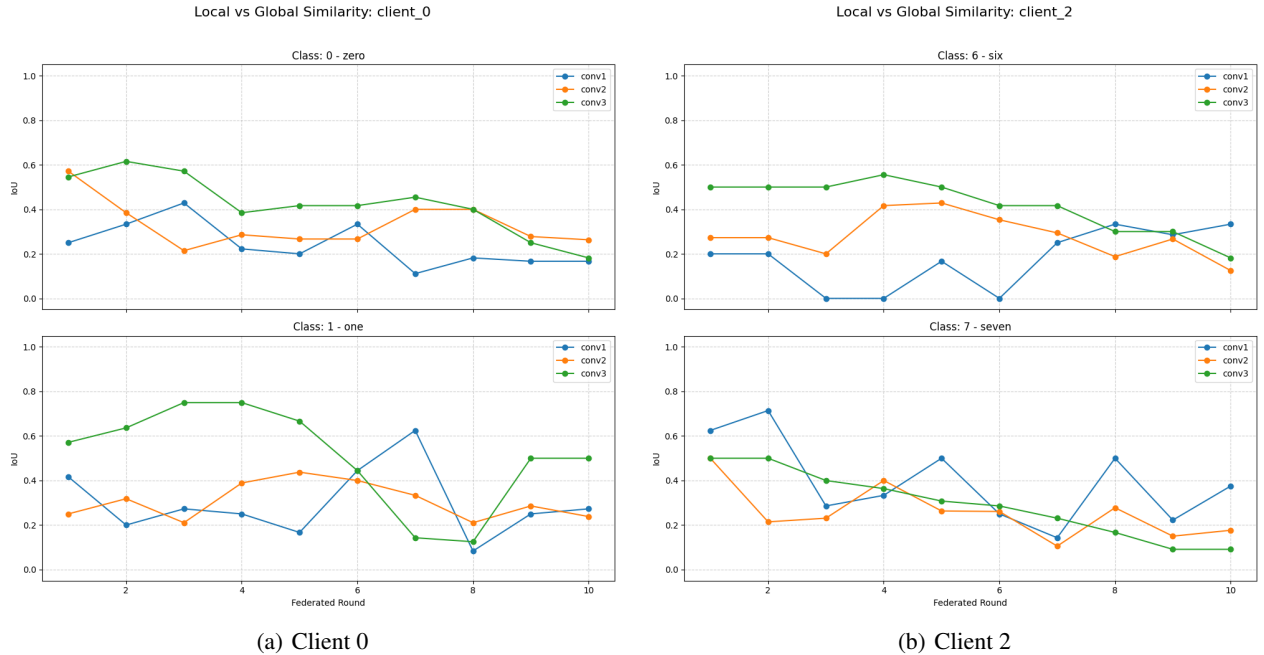


Figure 16. Supplementary Figure: Local vs. Global Circuit Similarity (Non-IID, 2-Class per Client). The structural collapse pattern persists in the 2-class per client setting. The trend holds for all clients and their respective specialized classes, showing that local circuits are not preserved in the global model.

A.3. Supplementary Figures for 3-Class Non-IID Experiment (50 Rounds)

The figures below show the local vs. global circuit similarity for all clients in the 50-round, 3-class-per-client experiment. The consistent pattern of low, noisy IoU across all clients supports the conclusion of persistent structural collapse presented in the main text.



Figure 17. Full Local vs. Global Circuit Similarity plots for the 3-Class per Client Non-IID experiment over 50 rounds.

A.4. Supplementary Figures for Shared Class Non-IID Experiment

The figures below show the local vs. global circuit similarity for each client in the "2 distinct, 1 shared" class experiment. The plots for the shared class ("0") show a trend towards higher and more stable IoU, approaching the behavior of the IID case. In contrast, the plots for the distinct classes show the low, noisy IoU characteristic of structural collapse.

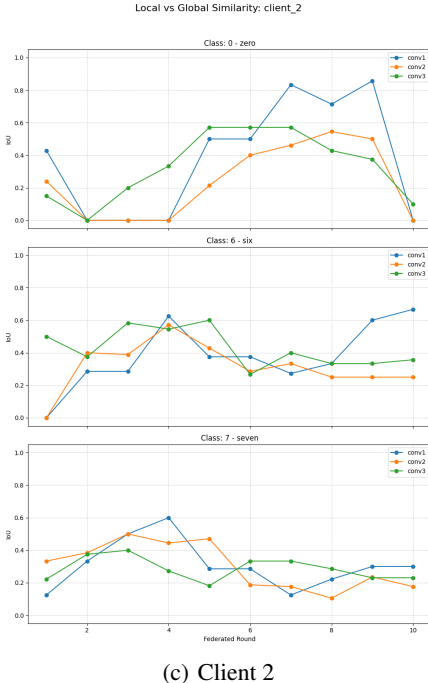
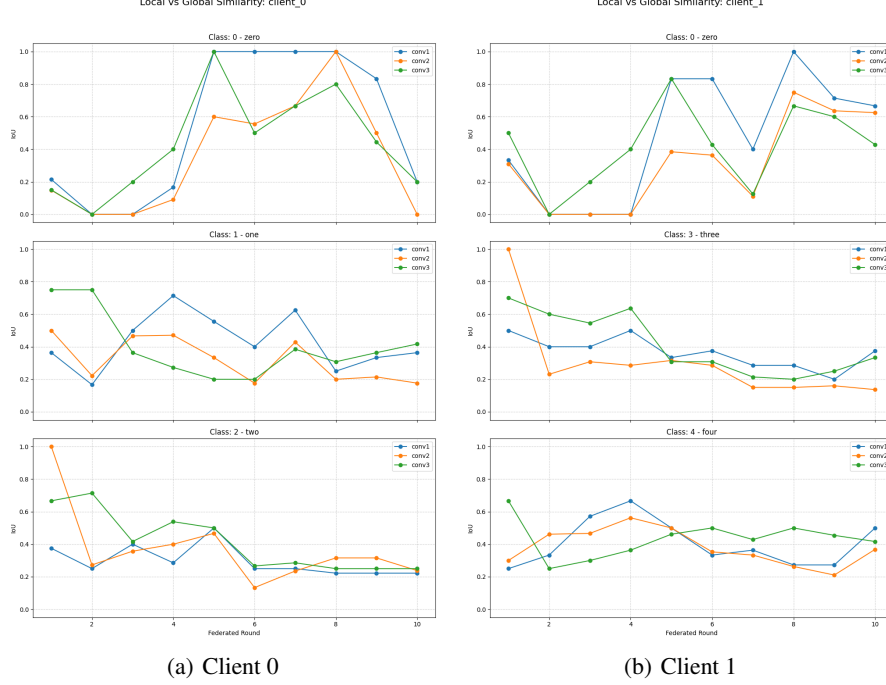


Figure 18. Full Local vs. Global Circuit Similarity plots for the Shared Class Non-IID experiment. Note the higher and more stable IoU for the shared class ("0") compared to the noisy IoU for the distinct classes.

A.5. Supplementary Figures for Sparsity Ablation Study

The figure below compares the functional stability (cross-evaluation accuracy) across four different weight sparsity levels in the 2-class-per-client Non-IID experiment. A clear trend is visible: as sparsity increases from 95% to 99.5%, the accuracy of the local masks on the global model becomes significantly more stable, with fewer and less severe drops to 0%. This supports the hypothesis that sparsity mitigates destructive interference.

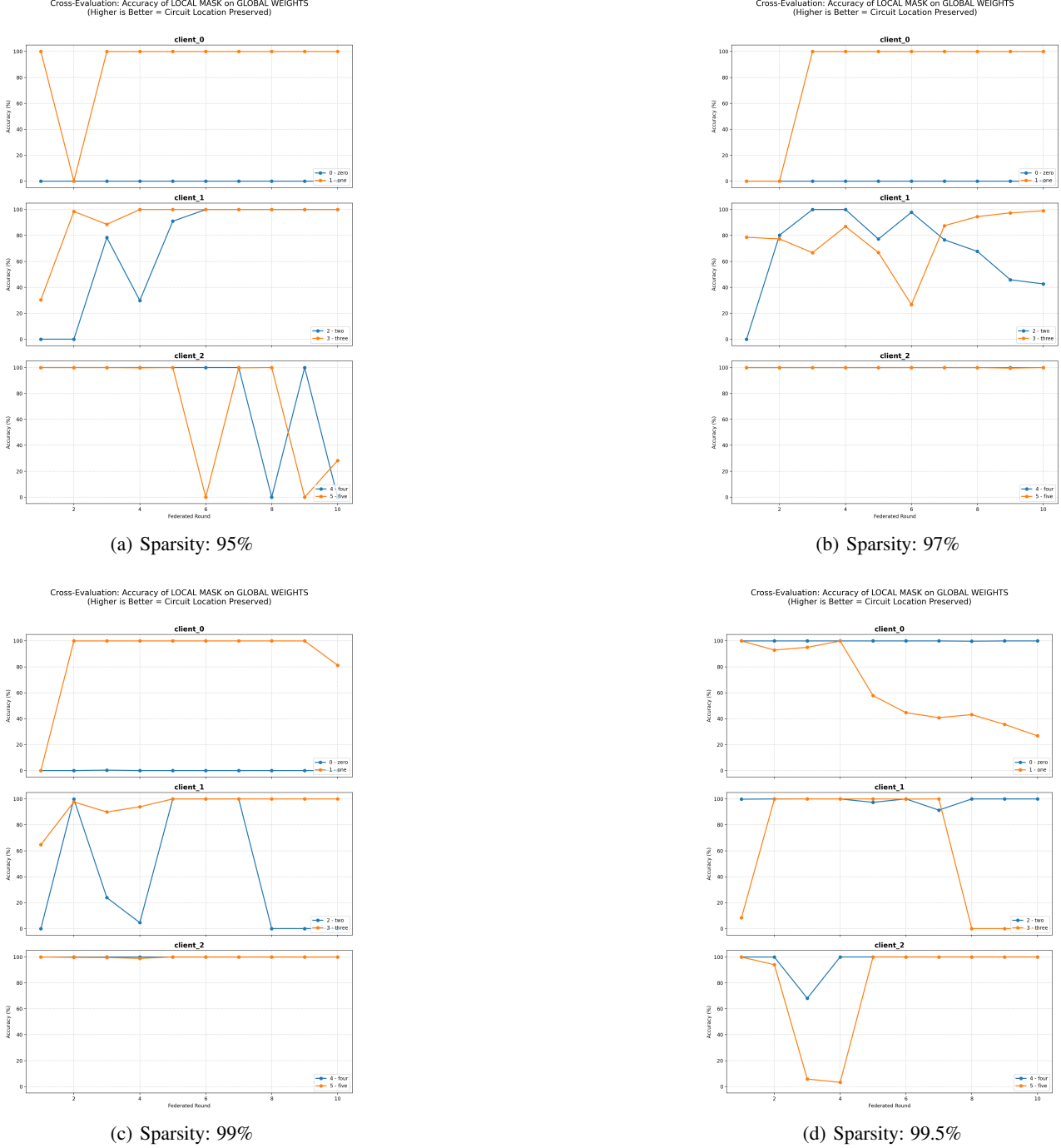


Figure 19. Sparsity Ablation: Cross-Evaluation Accuracy. Each panel shows the accuracy of local circuit masks on the global model for the 2-class Non-IID experiment at a different sparsity level. Higher sparsity clearly leads to more stable functional preservation.